

# UC Santa Barbara

## UC Santa Barbara Previously Published Works

### Title

Plate-Scale Imaging of Eastern US Reveals Ancient and Ongoing Continental Deformation

### Permalink

<https://escholarship.org/uc/item/4987g78q>

### Journal

Geophysical Research Letters, 51(12)

### ISSN

0094-8276

### Authors

Brunsvik, Brennan

Eilon, Zachary

Lynner, Colton

### Publication Date

2024-06-28

### DOI

10.1029/2024gl109041

### Copyright Information

This work is made available under the terms of a Creative Commons Attribution-NonCommercial-NoDerivatives License, available at

<https://creativecommons.org/licenses/by-nc-nd/4.0/>


Peer reviewed

# Geophysical Research Letters<sup>®</sup>

## RESEARCH LETTER

10.1029/2024GL109041

## Plate-Scale Imaging of Eastern US Reveals Ancient and Ongoing Continental Deformation

Brennan Brunsvik<sup>1</sup> , Zachary Eilon<sup>1</sup> , and Colton Lynner<sup>2</sup> 

<sup>1</sup>Department of Earth Science, University of California-Santa Barbara, Santa Barbara, CA, USA, <sup>2</sup>Department of Earth Sciences, University of Delaware, Newark, DE, USA

### Key Points:

- We present the highest resolution map to date of lithospheric properties from craton to margin in the eastern US
- Steep lithospheric steps drive edge-driven convection along the margin and influence modern topography
- Geologic boundaries correspond to plate-spanning changes in seismic properties, including a possible continental suture

### Supporting Information:

Supporting Information may be found in the online version of this article.

### Correspondence to:

B. Brunsvik,  
brennanbrunsvik@ucsb.edu

### Citation:

Brunsvik, B., Eilon, Z., & Lynner, C. (2024). Plate-scale imaging of eastern US reveals ancient and ongoing continental deformation. *Geophysical Research Letters*, *51*, e2024GL109041. <https://doi.org/10.1029/2024GL109041>

Received 1 MAR 2024

Accepted 1 JUN 2024

### Author Contributions:

**Conceptualization:** Brennan Brunsvik, Zachary Eilon, Colton Lynner

**Data curation:** Brennan Brunsvik, Zachary Eilon, Colton Lynner

**Formal analysis:** Brennan Brunsvik, Zachary Eilon

**Funding acquisition:** Zachary Eilon, Colton Lynner

**Investigation:** Brennan Brunsvik, Zachary Eilon, Colton Lynner

**Methodology:** Brennan Brunsvik, Zachary Eilon

**Project administration:** Zachary Eilon

**Resources:** Brennan Brunsvik, Zachary Eilon

**Software:** Brennan Brunsvik, Zachary Eilon

**Supervision:** Zachary Eilon

**Validation:** Brennan Brunsvik, Zachary Eilon

© 2024. The Author(s).

This is an open access article under the terms of the [Creative Commons Attribution License](https://creativecommons.org/licenses/by/4.0/), which permits use, distribution and reproduction in any medium, provided the original work is properly cited.

**Abstract** Eastern North America was constructed over several Wilson cycles, culminating in the breakup of Pangea. Previous seismological imaging lacked the resolution to depict precisely how ancient tectonic boundaries manifest throughout the lithosphere, how continental breakup modified the plate, or how ongoing mantle dynamics shapes the continental margin. We present a high-resolution, plate-scale seismic tomography model of the eastern US by combining an unprecedented suite of complementary data sets in a Bayesian framework. These data provide detailed resolution from crust to asthenosphere, identifying the base of the lithosphere and mid-lithospheric discontinuities. The plate thins in steps that align with ancient orogens. The lithospheric step at the Appalachian front is associated with cells of mantle upwellings, likely edge-driven convection, that erode the base of the plate and shape modern Appalachian topography. Low-velocity structures in the lithospheric-mantle align with the Grenville front and may be remnants of Rodinia assembly.

**Plain Language Summary** Eastern North America was constructed through several cycles of supercontinent assembly and breakup. The North American tectonic plate contains scars of this billion-year history, but previous seismological imaging lacked the resolution to identify leftover structures that elucidate past processes or shed light on contemporary ones. We have produced a high-resolution 3-D seismological image of the eastern North American plate. Our imaging method combines numerous complementary data sets, which together provide resolution from the surface to beneath the plate. The plate is thickest where it is oldest, in the continental interior. It thins progressively eastward in steps that align well with geologically defined boundaries, and is thinnest next to the Atlantic ocean. A sharp step in plate thickness beneath the Appalachian Mountains provokes small convection cells, as cold plate drops off and hotter material ascends to replace it, pushing up the Appalachian mountains. We find a well-preserved “fossil” of a collision zone, deep within the plate, likely left over from a billion-year old supercontinent formation. The most recent supercontinent breakup, which led to Atlantic opening, has left a legacy of thin and heavily modified plate east of the Appalachians.

## 1. Introduction

Eastern North America (ENA) has grown through collisional and subduction events (Whitmeyer & Karlstrom, 2007) (Figure 1). Proterozoic subduction and island arc accretion culminated in the Grenville orogeny and assembly of the supercontinent Rodinia (~1.3–0.9 Ga). Failed rift basins developed during and after Rodinia assembly, including the Rome Trough, leaving marks on the lithosphere. Rodinia broke up at ~0.6 Ga. The Appalachian orogeny and assembly of Pangea at ~450 Ma was followed by the ~200 Ma Central Atlantic Magmatic Province (CAMP), continental breakup, and opening of the Atlantic Ocean (Withjack et al., 2012). Since this time, eastern North America has been a passive margin (or “passive aggressive”; Mazza et al., 2017).

The Eastern North American Margin (ENAM) experienced intraplate tectonic activity (Biryol et al., 2016; Brunsvik et al., 2021) and has variable mantle seismic velocity structure (Savage, 2021; Wagner et al., 2018), including several slow anomalies. The Central Appalachian Anomaly (CAA) aligns with intraplate, non-plume volcanism (Long et al., 2021), while the Northern Appalachian Anomaly (NAA) is associated with extensive lithospheric modification and plume influence (Menke et al., 2016, 2018; Tao et al., 2021). A long-standing question in ENA tectonophysics is why topography persists in the Appalachians (reaching up to 2 km), despite the margin being passive since nearly 200 Ma (Miller et al., 2013; Figure 1). Uplift, seismic velocity anomalies, anisotropy, and intraplate volcanism are attributed to contemporary mantle dynamics, including shear-driven upwelling, edge-driven convection, and/or delamination of thick lithosphere (Long et al., 2021; Menke et al., 2018).

**Visualization:** Brennan Brunsvik,  
Zachary Eilon  
**Writing – original draft:**  
Brennan Brunsvik, Zachary Eilon  
**Writing – review & editing:**  
Brennan Brunsvik, Zachary Eilon,  
Colton Lynner

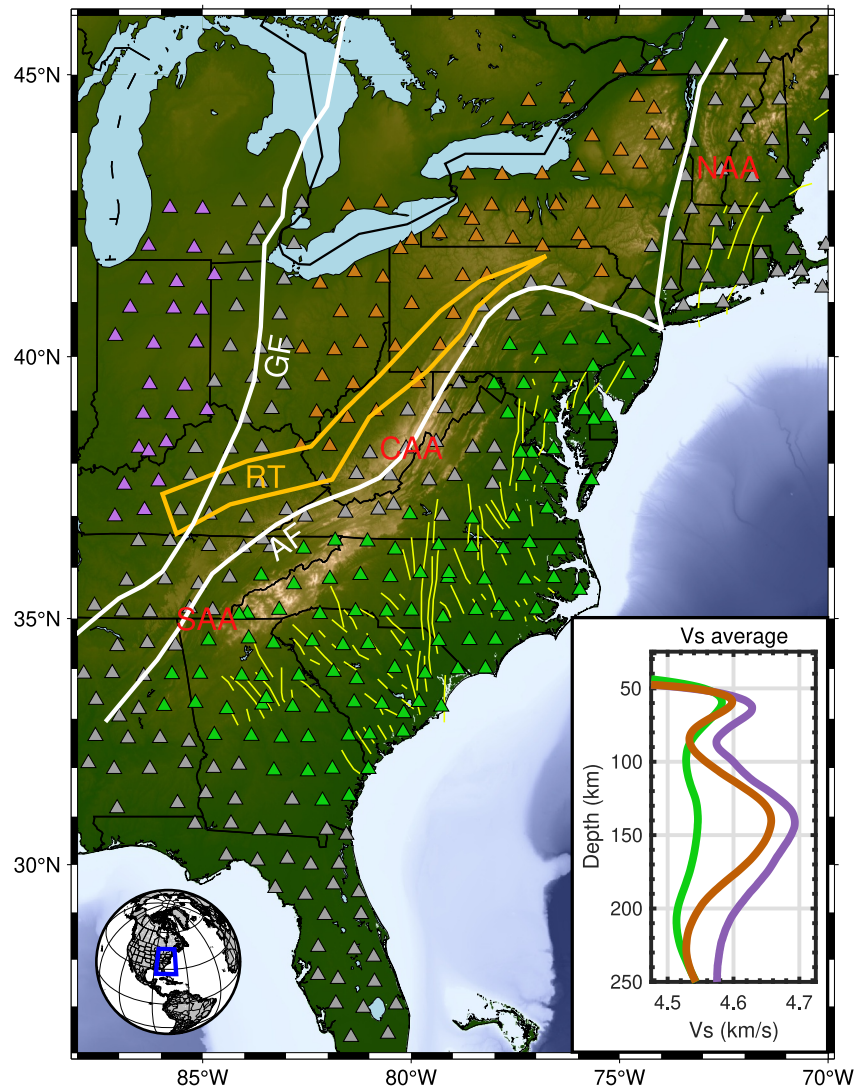


**Figure 1.** Map of study area. Triangles show seismic stations used for inversion. Bottom right: average velocity profiles for three regions (*Granite-rhyolite province (GRP)* in purple, *Grenville* in brown, and *Margin* in green). Stations in these regions are also color coded, others are gray. Yellow lines: CAMP dikes (Jourdan et al., 2009; Shen & Ritzwoller, 2016). RT: Rome-Trough Rift. GF: Grenville Front. AF: Appalachian Front. S/C/NAA: Southern/Central/Northern Appalachian Anomalies.

Across ENA tectonic boundaries, lithospheric structure remains unclear. The lithosphere-asthenosphere boundary (LAB) has depth estimates in the Piedmont and coastal plains ranging from 70 km (Hopper & Fischer, 2018) to 200 km (Murphy & Egbert, 2019), blurring interpretations of tectonic history and mantle dynamics. Further, scattered wave studies observe mid-lithospheric velocity discontinuities (MLDs)—abrupt intraplate drops in seismic velocity that are easily confused with the LAB—at ~70–100 km depth (Hopper & Fischer, 2018). MLDs may be geochemically distinct layers related to past subduction, metasomatic infiltration, or in situ melt (Selway et al., 2015). Finally, while the Grenville front is intermittently mapped from surface exposures, borehole data, gravity, and magnetics (Mosher, 1998; Stein et al., 2018; Whitmeyer & Karlstrom, 2007), it is not exposed through much of the US. Grenville thrusts have been identified in the US crust (Culotta et al., 1990; Hopper et al., 2017; Long et al., 2019), but no associated feature has previously been observed in the lithospheric mantle.

We conducted seismic tomography to identify tectonic structures and infer mantle processes across ENA from margin to craton (Figures 2 and 3). Surface wave dispersion constrains absolute velocity with coarse depth resolution, while receiver functions precisely depict depths and amplitudes of velocity gradients. Together, these complementary data (e.g., Bodin et al., 2012) enable lithosphere-scale imaging (Sections S1, S2, and S3 in

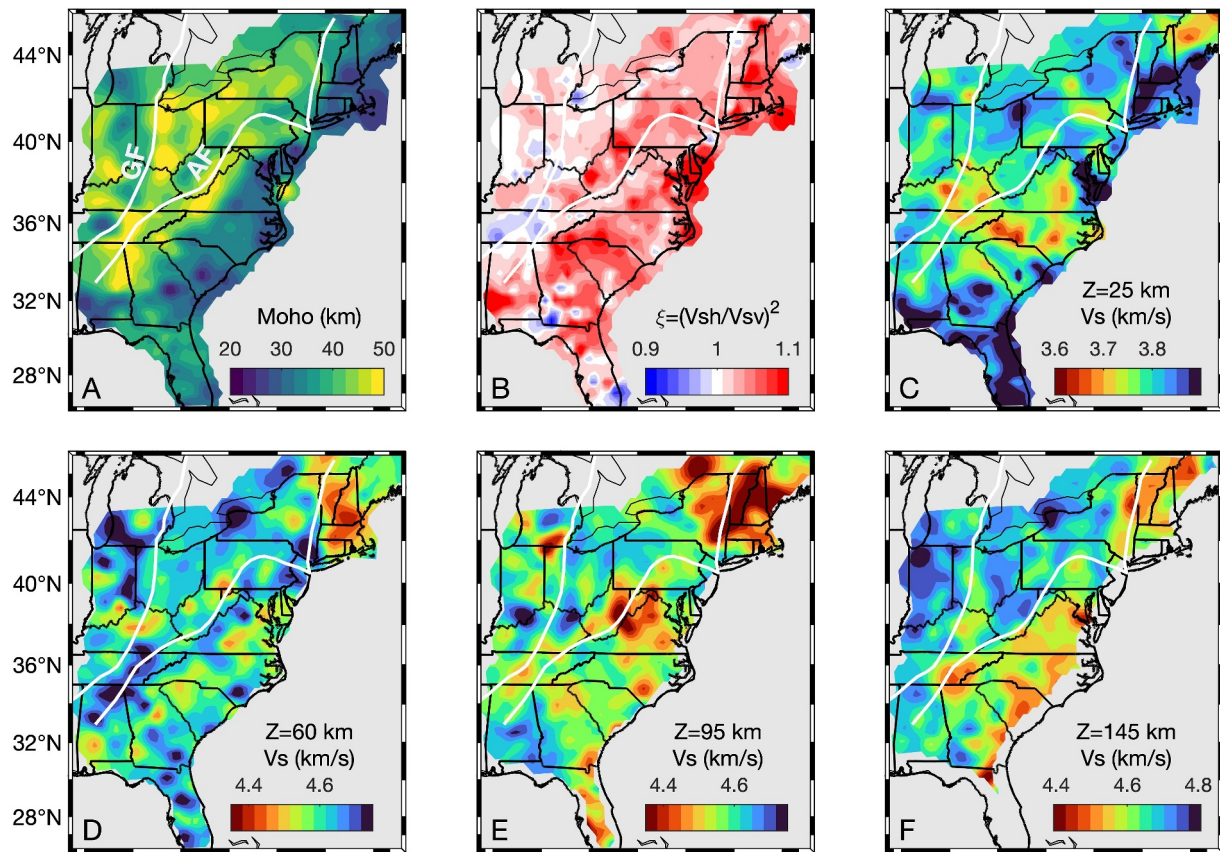


**Figure 2.** Map-views of model. (a) Moho depth. (b) Radial anisotropy  $\xi = V_{SH}^2/V_{SV}^2$ . (c)–(f) Inverted velocity model at different depths. GF: Grenville Front. AF: Appalachian Front.

Supporting Information S1) with demonstrably improved resolution (Eilon et al., 2018; Petruska & Eilon, 2022; Shen & Ritzwoller, 2016). In this study, we obtained unprecedentedly detailed images of the LAB, MLDs, crustal structure, and mantle velocities. We used a unique combination of *S<sub>p</sub>* receiver function CCP stacks, *P<sub>s</sub>* receiver functions, and several surface wave data sets inverted in a Bayesian framework (Methods, Sections S4 and S5 in Supporting Information S1). Our models depict detailed 3-D variations in plate properties across ENA, from crust to asthenosphere.

## 2. Methods

### 2.1. Inversion Approach

Our approach follows Eilon et al. (2018), based on well-established principles for joint inversion of surface and scattered waves (Bodin et al., 2012; Shen & Ritzwoller, 2016). We jointly invert an unprecedentedly comprehensive suite of published data sets spanning ENA. These include Rayleigh and Love wave data (including from shoreline-crossing studies), and both *P<sub>s</sub>* and *S<sub>p</sub>* information. We use a Markov-Chain Monte-Carlo (MCMC) inversion that conducts importance sampling to estimate a model parameters' probability density functions (PDFs), solving at each station for 1-D shear velocity profiles, Moho and sediment depths, average crustal  $V_p/V_s$ , and crustal radial anisotropy  $\xi = V_{SH}^2/V_{SV}^2$ . Sections S1 and S2 in Supporting Information S1 explains updates to the methodology from Eilon et al. (2018), including use of radially anisotropic *H*- $\kappa$  stacks (Brunsvik & Eilon, 2023), *S*-*p* receiver functions extracted from Common Conversion Point (CCP) volumes, Rayleigh wave ellipticity, and simultaneous incorporation of multiple studies' phase velocity dispersion curves. The Data Availability Statement and Section S2 in Supporting Information S1 describe our data sets, and Section S2.4 in Supporting Information S1 explains our forward calculations. Synthetic tests demonstrate that features are recovered with accuracy and precision sufficient to support the observations discussed below, particularly

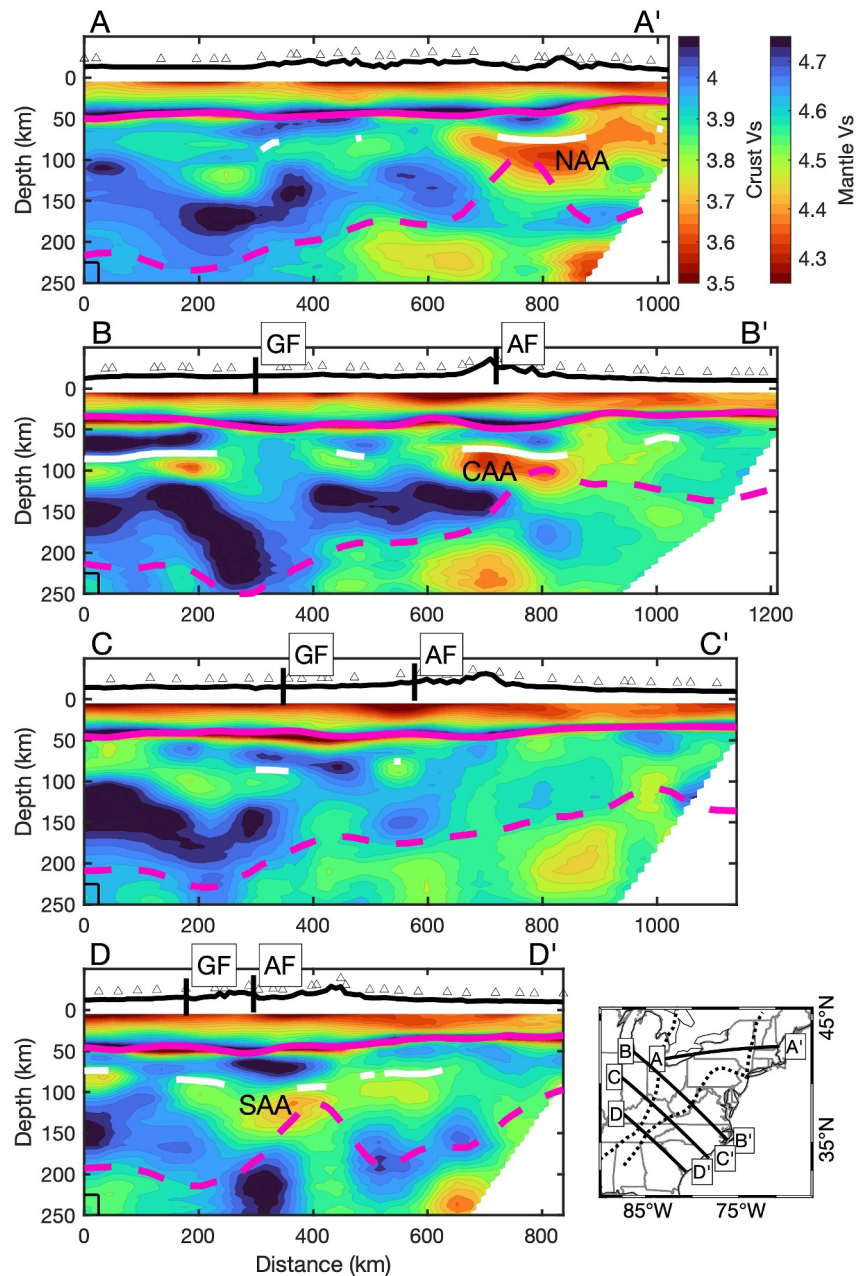


**Figure 3.** Cross-sections of tomographic model. Section locations shown at bottom right. Black triangles are stations, projected onto section. Topography, in black, has 20x vertical exaggeration, shifted up 10 km. Moho is solid magenta line. LAB is magenta dashed line, and MLDs (plotted where detected) are solid white lines at the shallower velocity gradient of the features. Bottom left of each plot has a square box (25 km × 25 km) showing (mild) vertical exaggeration. Note the different color scales for crust and mantle velocities. GF: Grenville Front. AF: Appalachian Front. S/C/NAA: Southern/Central/Northern Appalachian Anomalies.

pertaining to Moho depth, MLDs, and the LAB (Section S3 in Supporting Information S1). We provide error estimates for the models, and only discuss features required by the data (Section S6 in Supporting Information S1).

## 2.2. Model Processing

From 1-D velocity profiles, we produce a 3-D velocity volume by fitting smooth isovelocity contours that maximize global likelihood of all stations' posterior PDFs (Section S5 in Supporting Information S1). We then

calculate temperature from shear velocity (Section S7 in Supporting Information S1). We assume Iherzolite mantle and use a thermodynamic calculator (Abers & Hacker, 2016) to compute mineralogy and anharmonic moduli, and then apply the “pre-melting” model (Yamauchi & Takei, 2016) to account for anelastic effects. We ignore melt and hydration, and hold grain-size and composition constant. We map the LAB as the 1150°C isotherm, trusting more in relative than absolute depths (see Section S7 in Supporting Information S1). We compute two metrics for lithospheric thickness and temperature: the average mantle velocity above 250 km (“*avV*”) and the integral of the mantle velocities exceeding 4.5 km/s (i.e., combining wavespeed and thickness into one number: “*fastlith*”).

### 3. Results and Discussion

#### 3.1. Progressively Thinned Lithosphere Records Tectonic History

To understand first-order mantle structure, we inspect average velocity profiles and properties of three clearly distinct regions: “*Margin*” (primarily the Piedmont and coastal plains), “*Grenville*” (between the Grenville Front and Appalachian Front), and the Granite Rhyolite Province, or “GRP,” west of the Grenville Front (Figure 1). Velocity is highest toward the craton (cf. Nettles & Dziewoński, 2008). The GRP has the fastest average velocities (mean of 4.65 km/s, peak of 4.72 km/s) and thickest lithosphere: ~210 km (Figure 4), based on thermal modeling (Section S7 in Supporting Information S1). The GRP’s integrated relative lid velocity (“*fastlith*”; Section S7 in Supporting Information S1) is 1.77x greater than the Late Proterozoic global average (Figure 3). On the other side of the Grenville front, the *Grenville* region’s LAB is at an average depth of 185 km (c.f. ~190 km in Fullea et al., 2021). The *Grenville fastlith* value is 1.34x greater than the Late Proterozoic average. Interpreted in terms of temperature in the mid-lithosphere (150 km depth), this translates to ~100 K warmer than the GRP region (Section S7 in Supporting Information S1). These regions have relatively thick crust, ~42 km.

The *Margin* looks quite different and records the effects of Jurassic continental breakup. Much of this area lacks a clear fast mantle below ~100 km depth, suggesting the lithosphere here is thin (the 1150°C isotherm gives 130 km on average, similar to 140 km in Fullea et al., 2021) and/or unusually warm (~1160°C at 150 km depth, 300 K hotter than the *Grenville*). The *Margin* crust is also notably thinner than the continental interior ~34 km on average. Moreover, while the GRP and *Grenville* regions show no clear crustal radial anisotropy, the *Margin* region has widespread strong  $V_{SH} > V_{SV}$  anisotropy ( $\xi \sim 1.07$ ), consistent with previously inferred extensional fabrics (Brunsvik et al., 2021). The *Margin*’s slowest upper mantle coincides closely with the distribution of CAMP dykes, suggesting that the CAMP’s thermal legacy persists today (Figure 1).

Our inferred plate thickness and thermo-elastic properties agree well with elastic thicknesses here (Audet & Bürgmann, 2011; Tesaro et al., 2015), and the stair-step gradient of lithospheric thinning we see matches independently constrained mechanical anisotropy (Audet & Bürgmann, 2011). Our findings, particularly the long-lived thermal effect of CAMP and extensional strain fabrics, support the idea of inherited weakness as a dominant control on continental dynamics across Wilson cycles (Thomas, 2006).

#### 3.2. Ancient Orogens Control Present-Day Dynamics

Tectonic features are preserved in the lithosphere (Levin et al., 2017), and shown in our models. At the surface-mapped location of the Grenville front (GF) (Whitmeyer & Karlstrom, 2007), we observe thick (~50 km) crust and a decrease in mantle  $V_S$  (~0.2 km/s at 145 km depth; Figure 2). This region of depressed velocities spans >700 km along the front, from ~35°N to ~42°N, and dips steeply eastwards from the surface to the ~200 km base of the lithosphere (Figure 3, B-B’), although precise dip is not well constrained. We suggest this represents a preserved contractional Grenville orogenic structure through the lithosphere, possibly from lithospheric imbrication (Chen et al., 2018; Hinze & Chandler, 2020). Crustal Grenville thrusts have been imaged with much shallower dip, reaching the Moho as far as 400 km east of the GF (Culotta et al., 1990; Long et al., 2019). Reconciling these crustal features with the sub-vertical mantle suture imaged here requires crust and mantle decoupling during continental collision (Lin et al., 2023). At the Appalachian front (AF), a more profound lithospheric shift is observed. At ~145 km depth, velocity decreases markedly stepping east across the AF, from ~4.70 to ~4.55 km/s on average (Figure 2). This velocity drop extends along the AF from ~35°N to 45°N, with strong correlation to surface expressions of the Appalachian orogen. There is a concomitant 85 km drop in lithospheric thickness over just 145 km in horizontal distance, implying an LAB dip of ~30°.

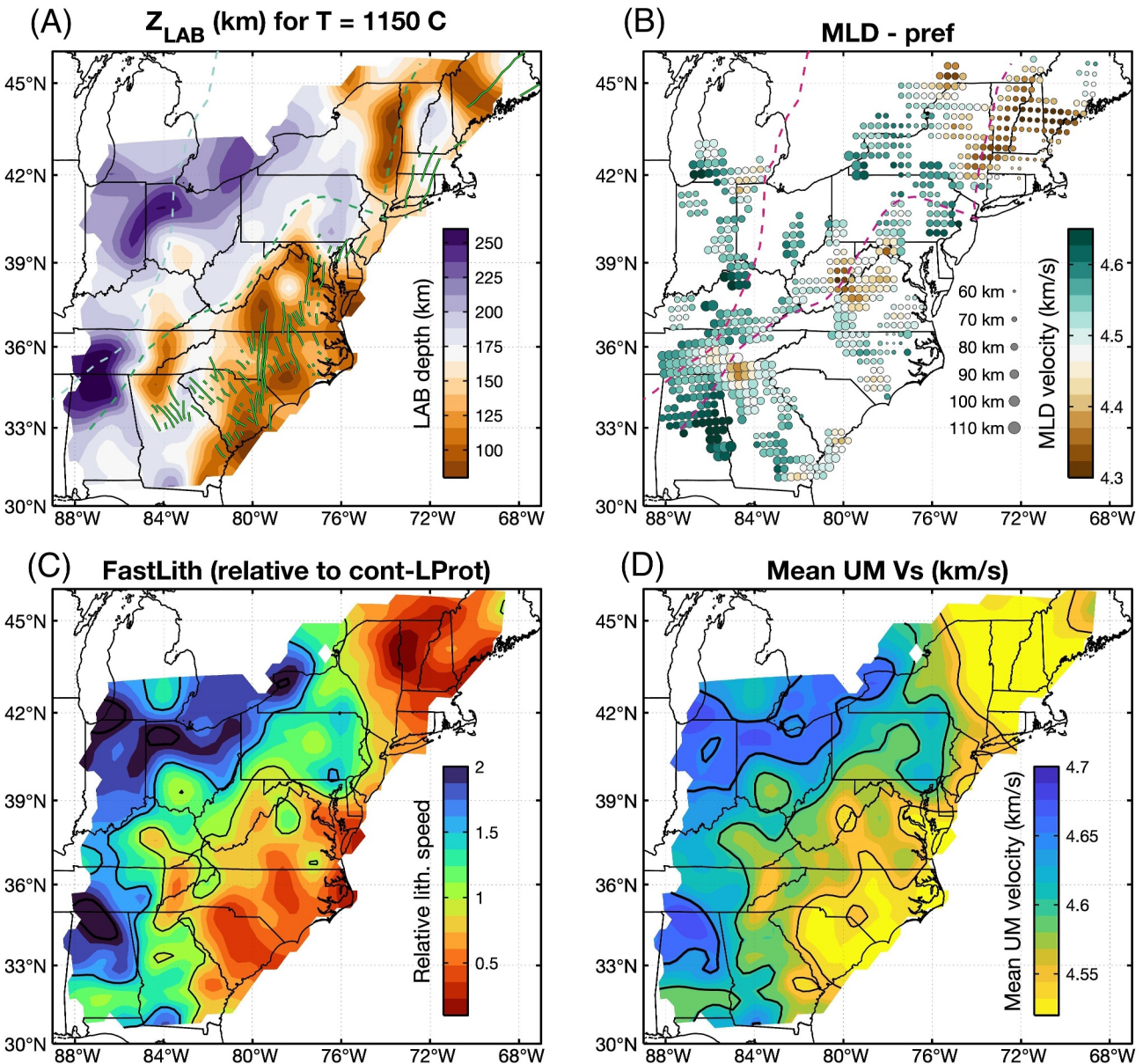


**Figure 4.** Maps depicting lithospheric properties. (a) LAB depth from the estimated 1150°C isotherm. Dashed lines show Grenville Front (lighter green, further NW) and Appalachian Front (darker green, further SE). Green solid lines show CAMP dikes (Jourdan et al., 2009). (b) MLD properties at all points where an MLD was detected. Point size corresponds to the depth of the negative velocity gradient, and color indicates the low-velocity layer minimum velocity. (c) The *fastlith* property, expressed relative to the value for globally averaged continental Late Proterozoic crust (Section S7 in Supporting Information S1), with thick contours at 1, 1.5, and 2. (d) The average shear velocity between the Moho and 250 km depth, with black contours at 4.55, 4.60, and 4.65 km/s.

We find three spatially localized, upper mantle low-velocity anomalies along the Appalachians: the NAA, CAA and Southern Appalachian anomaly (SAA) at the Georgia-Tennessee border (Figure 2). The SAA, a deeper (130 km) but statistically significant (Section S6; Figure S16 in Supporting Information S1)  $\sim 4.5\%$  slow feature, is missing in some tomography models (e.g., Shen & Ritzwoller, 2016), and present in others (e.g., Brunsvik et al., 2021; Schmandt & Lin, 2014). The NAA and CAA are more widely observed (Carrero Mustelie & Menke, 2021; Dong & Menke, 2017; Shen & Ritzwoller, 2016), perhaps because they are shallower. Each anomaly has thinned lithosphere, slow MLDs, and is juxtaposed against thicker lithosphere to the NW. For instance, the CAA is 4%–5% slower in  $V_s$  than ambient surrounding lithosphere at 95 km depth (Figures 2 and 3) consistent with hot mantle (1460–1510°C) and in situ melt fraction of  $\sim 2.5\%$  (Savage, 2021) (Section S7 in Supporting Information S1). Given our smooth parameterization, we likely underpredict velocity extrema, so melt

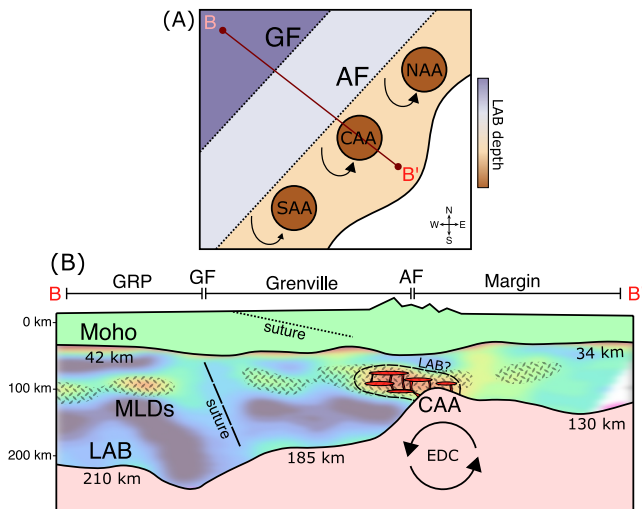


**Figure 5.** Summary of observations and interpretations. (a) Distinct lithospheric regions separated by geologic boundaries, with North/Central/Southern Appalachian Anomalies (N/C/SAA) related to mantle upwellings east of the Appalachian front, AF. (b) Cross section spanning from craton to margin. Edge-driven convection (EDC) shown beneath the associated CAA. Grenville sutures shown as dashed lines in the mantle (from our imaging) and crust (from Long et al., 2019). Low velocity mid-lithospheric discontinuities (MLDs) are schematically illustrated with hatches as metasomatized material. Melt shown at CAA, either below or above the LAB. Average Moho and LAB depth values from Figure 4 section B-B'. GF: Grenville Front. AF: Appalachian front. GRP: *Granite-Rhyolite province*. LAB: Lithosphere-asthenosphere boundary.

~175 km depth dimension of the convective system, and matches some numerical model predictions (Ramsay & Pysklywec, 2011). Since the CAA and SAA are relatively isolated pockets of abruptly thinned lithosphere, shear-driven upwelling (Conrad et al., 2010) may also play a role.

The Appalachian front is just oceanward of the Rome Trough, a failed rift (Figure 1), where we find among the highest lithosphere velocities (4.76 km/s at 145 km). Depletion from rifting can increase the Mg#, decrease mantle density, and increase seismic velocity (Schutt & Leshner, 2006), while strengthening the plate by reducing the fraction that is crust. Lower density lithosphere is more resistant to erosion from EDC (Liu & Chen, 2019). We posit that strong, fast lithosphere associated with the failed Rome Trough rift may have provided a backstop for the Appalachian orogeny, and currently acts to localize edge-driven convection at, and eastward of, the AF.

Both Grenville and Appalachian fronts exhibit thickened crust (c.f. Levin et al., 2017) to ~50 km (Figure 2). However, only the Appalachians have high topography (Figure 1). Our models show the Appalachians are underlain by thinner lithosphere (as shallow as ~90 km). Thus simple isostasy may explain high Appalachian topography (in conjunction with dense crustal roots; Fischer, 2002). In fact, isostatic balance between the Appalachian front and the GRP region, using densities and depths inferred from our models, predicts ~4.5 km elevation (Section S8 in Supporting Information S1), markedly over-estimating observed Appalachian topography. The elastic plate evidently diminishes and distributes the excess topography regionally. Mantle upwellings and dynamic topography may further support high elevations (Ramsay & Pysklywec, 2011). By contrast, at the Grenville front, thick crust is matched by ~50 km of lithospheric thickening (Figure 4, B-B'). Similar isostatic calculations at the Grenville front predict no topographic excess, matching observations. Ultimately, elevated topography in the Appalachians is an isostatic response to thin lithosphere under thick crust.

### 3.3. Chemical and Melt Layers in the Mid-Lithosphere

We observe widespread mid-lithospheric discontinuities (MLDs) in our model (Figures 3 and 4). These mostly correspond to *Sp* phase conversions from negative velocity gradients at the top of intra-lithospheric low velocity layers (LVLs). MLDs are sufficiently ubiquitous in the GRP and *Grenville* regions to produce a velocity

percentages may be locally higher than stated here. Our lowest velocities span ~70~145 km depth, but body-wave tomography suggests slow wavespeed may extend to ~400 km (Biriyol et al., 2016; Brunsvik et al., 2021).

Multiple lines of evidence, including velocity tomography, receiver functions, magnetotellurics, and seismic attenuation, support our conclusion that these anomalies have thinned lithosphere and/or partial melt, suggestive of upwelling (Long et al., 2021). We interpret these anomalies as sites of edge-driven convection at the LAB gradient (Figure 5). This process explains ongoing mantle flow (King & Ritsema, 2000; Long et al., 2021; Lynner & Bodmer, 2017) and even lithospheric erosion (Liu & Chen, 2019). Edge-driven convection has three key hallmarks: (a) low-velocity upwellings, (b) high-velocity downwellings, and (c) a lithospheric step potential gradient. Our models clearly depict (a) and (c). The steeply dipping LAB at the AF is particularly striking. We may also observe (2) (e.g., beneath the Appalachian Front in Figure 3d).

While these mantle anomalies may have initially formed by other processes such as hot spots (Tao et al., 2021), edge-driven convection supplies warm upwelling mantle today. Our models provide new fodder for geodynamic studies of this complex process; the lithospheric profile, rheology, and plate-speed must all influence flow geometry, including along-strike segmentation (Afonso et al., 2016; Duvernay et al., 2021; Liu & Chen, 2019; Ramsay & Pysklywec, 2011). Previous workers discuss individual EDC cells (Levin et al., 2018; Menke et al., 2018), and our models suggest EDC is a highly 3-D process along the margin. LAB topography provides a mostly SE-NW gravity potential gradient. Linear stability analysis predicts an NE-SW segmentation of convective cells due to differential anomaly growth rate (Turcotte & Schubert, 2014). The ~500 km separation of these anomalies implies a



minimum in these regions' average velocity profiles (Figure 1). We map MLD depths and associated velocity minima in our models (Figure 4; Methods; Section S7 in Supporting Information S1). While all MLDs are found in a similar depth range—between ~60 and 100 km—they have varying characteristics and apparent underlying mechanisms (Selway et al., 2015). West of the Appalachian front, MLDs are mostly fast ( $>4.5$  km/s LVLs), mostly deeper ( $>80$  km), and mostly record  $<3\%$  velocity reductions. We interpret these as owing to chemical heterogeneities from metasomatism of older lithosphere; metasomatism through reasonable quantities of par-gasite and phlogopite can produce these  $<3\%$  velocity reductions (Saha et al., 2021).

By contrast, several areas east of the AF show larger velocity reductions,  $>4.5\%$ , and slow absolute velocities,  $<4.45$  km/s LVLs. These predominantly coincide with the NAA (MLD depth ~70 km, ~3–6% slow), CAA (MLD depth ~80 km, ~5% slow), and SAA (MLD depth ~95 km, ~6.5% slow). The slowest velocities are incommensurate with even a heavily metasomatized lithology. It is possible that these result from thermally triggered anelastic dissipation due to elastically accommodated grain-boundary sliding (Karato et al., 2015). However, these features are spatially confined, and it is difficult to imagine why this anelastic mechanism would appear so locally. Heat alone does not lower the velocity by more than ~5% before the solidus is reached (Petruska & Eilon, 2022). Thus, we interpret these distinctly slow anomalies as signatures of small-fraction partial melt within the lithosphere. Notably, the top of the CAA MLD matches the depth of co-located Eocene mantle melts (Mazza et al., 2014). At the N/C/SAA, we infer connectivity between localized sub-plate processes (chiefly edge-driven convective cells) and intraplate modification. This requires some transport of melts through the lower portion of the plate, perhaps by impounding (Havlin et al., 2013). The NAA/CAA could come from melt percolating or ponding in lithosphere, or replacement of lithosphere with asthenosphere (Figure 5).

North of  $38^{\circ}\text{N}$ , we find MLDs west of the Grenville front that largely disappear across the front (Figure 4 B-B'). Some workers have suggested that chemical MLDs are primarily situated at the edges of cratons (Krueger et al., 2021). Our results are consistent with that idea, but not dispositively so; little of the Superior cratonic interior is covered by our study and thus a statistical analysis of MLD predisposition toward craton margins is not possible. East of the Grenville Front, however, most MLD locations are not clearly related to tectonic fronts. This implies that they largely owe to processes more recent than the continent-building orogenies, bolstering our case that active mantle dynamics shape much of plate-scale structure today.

## 4. Conclusion

We jointly inverted multiple seismic datatypes for a lithosphere-spanning velocity model of eastern North America, including maps of LAB and MLD depths and properties. The plate thins in steps aligned with ancient orogens. A steep LAB gradient at the Appalachian front coincides with three mantle upwellings, likely due to edge-driven convection, that shape the base of the plate and modern Appalachian topography. A low-velocity structure in the lithospheric-mantle at the Grenville front may be a remnant of Rodinia assembly, shedding light on relative deformation of crust and mantle during orogeny. Based on the velocities of detected MLDs, we interpret them as metasomatized material and occasionally partial melt.

## Data Availability Statement

Our MCMC code is available at [https://github.com/brennanbrunsvik/THBI\\_MCMC](https://github.com/brennanbrunsvik/THBI_MCMC). Our tomography models are available via Zenodo repository [10.5281/zenodo.8241965](https://zenodo.org/record/8241965) (Brunsvik et al., 2023). *P<sub>s</sub>* receiver function data was obtained from the EarthScope DMC. Other data sets for this research are available in the citations below. We jointly invert an unprecedentedly comprehensive suite of data sets spanning ENA. We used continent-spanning phase velocity measurements (Section S2.1 in Supporting Information S1) from ambient-noise Love (6–40 s) and Rayleigh (5–40 s) waves (Ekström, 2017), earthquake Rayleigh waves (25–180 s) (Babikoff & Dalton, 2019), and HV ratios (16–90 s) (Shen & Ritzwoller, 2016). We also used *S<sub>p</sub>* receiver functions from CCP stacks (Hopper & Fischer, 2018) (Section S2.2 in Supporting Information S1), and *H–κ* stacks from the EARS *P<sub>s</sub>* receiver functions, reprocessed to account for radial anisotropy (Brunsvik & Eilon, 2023; Crotwell & Owens, 2005; Incorporated Research Institutions for Seismology, 2010) (Section S2.3 in Supporting Information S1). To optimally capture structure right up to the continent-ocean transition, we included local phase velocity data sets from the ENAM Community Seismic Experiment broadband data set that add shoreline-crossing constraints, including the

ambient noise (8–32 s) (Lynner & Porritt, 2017) and earthquake (25–100 s) (Lynner et al., 2019) Rayleigh wave phase velocities (also available in our Zenodo repository [10.5281/zenodo.8241965](https://zenodo.org/record/8241965)). Supporting Information S1 includes detailed method descriptions, synthetic tests, descriptions of data sets, detailed results at example US station CEH, 3-D velocity inversion, temperature modeling, LAB depth, MLD depth, and isostasy calculations.

#### Acknowledgments

We used UCSB CNSI computing, supported by NSF CNS-1725797 and DMR 2308708. This work was funded by NSF OCE 1753722 (ZE) and OCE 2001145 (CL). We thank Eva Golos and Karen Fischer for their contributions to the MCMC method.

#### References

- Abers, G. A., & Hacker, B. R. (2016). A MATLAB toolbox and Excel workbook for calculating the densities, seismic wave speeds, and major element composition of minerals and rocks at pressure and temperature. *Geochemistry, Geophysics, Geosystems*, *17*(2), 616–624. <https://doi.org/10.1002/2015gc006171>
- Afonso, J. C., Rawlinson, N., Yang, Y., Schutt, D. L., Jones, A. G., Fulla, J., & Griffin, W. L. (2016). 3-D multiobservable probabilistic inversion for the compositional and thermal structure of the lithosphere and upper mantle: III. Thermochemical tomography in the western-central U.S. *Journal of Geophysical Research: Solid Earth*, *121*(10), 7337–7370. <https://doi.org/10.1002/2016JB013049>
- Audet, P., & Bürgmann, R. (2011). Dominant role of tectonic inheritance in supercontinent cycles. *Nature Geoscience*, *4*(3), 184–187. <https://doi.org/10.1038/ngeo1080>
- Babikoff, J. C., & Dalton, C. A. (2019). Long-period Rayleigh wave phase velocity tomography using USArray [Dataset]. *Geochemistry, Geophysics, Geosystems*, *20*(4), 1990–2006. <https://doi.org/10.1029/2018GC008073>
- Biryol, C. B., Wagner, L. S., Fischer, K. M., & Hawman, R. B. (2016). Relationship between observed upper mantle structures and recent tectonic activity across the Southeastern United States. *Journal of Geophysical Research: Solid Earth*, *121*(5), 3393–3414. <https://doi.org/10.1002/2015JB012698>
- Bodin, T., Sambridge, M., Tkalčić, H., Arroucau, P., Gallagher, K., & Rawlinson, N. (2012). Transdimensional inversion of receiver functions and surface wave dispersion. *Journal of Geophysical Research*, *117*(B2). <https://doi.org/10.1029/2011JB008560>
- Brunsvik, B., & Eilon, Z. (2023). Radial anisotropy in receiver function h- $\kappa$  stacks. *Seismological Research Letters*, *95*(1), 479–487. <https://doi.org/10.1785/022022030114>
- Brunsvik, B., Eilon, Z., & Lynner, C. (2023). Plate-scale imaging of eastern US reveals ancient and ongoing continental deformation [Dataset]. *Zenodo*. <https://doi.org/10.5281/zenodo.8241966>
- Brunsvik, B. R., Eilon, Z. C., & Lynner, C. (2021). Mantle structure and flow across the continent-ocean transition of the eastern North American margin: Anisotropic S-wave tomography. *Geochemistry, Geophysics, Geosystems*, *22*(12). <https://doi.org/10.1029/2021GC010084>
- Carrero Mustelie, E., & Menke, W. (2021). Seismic anomalies in the southeastern North American asthenosphere as characterized with body wave travel times from high-quality teleseisms. *Tectonophysics*, *809*, 228853. <https://doi.org/10.1016/j.tecto.2021.228853>
- Chen, C., Gilbert, H., Fischer, K. M., Andronicos, C. L., Pavlis, G. L., Hamburger, M. W., et al. (2018). Lithospheric discontinuities beneath the U.S. Midcontinent – Signatures of Proterozoic terrane accretion and failed rifting. *Earth and Planetary Science Letters*, *481*, 223–235. <https://doi.org/10.1016/j.epsl.2017.10.033>
- Conrad, C. P., Wu, B., Smith, E. I., Bianco, T. A., & Tibbetts, A. (2010). Shear-driven upwelling induced by lateral viscosity variations and asthenospheric shear: A mechanism for intraplate volcanism. *Physics of the Earth and Planetary Interiors*, *178*(3–4), 162–175. <https://doi.org/10.1016/j.pepi.2009.10.001>
- Crotwell, H. P., & Owens, T. J. (2005). Automated receiver function processing. *Seismological Research Letters*, *76*(6), 702–709. <https://doi.org/10.1785/gssrl.76.6.702>
- Culotta, R. C., Pratt, T., & Oliver, J. (1990). A tale of two sutures: COCORP's deep seismic surveys of the Grenville province in the eastern U.S. Midcontinent. *Geology*, *18*(7), 646. [https://doi.org/10.1130/0091-7613\(1990\)018<0646:ATOTSC>2.3.CO;2](https://doi.org/10.1130/0091-7613(1990)018<0646:ATOTSC>2.3.CO;2)
- Dong, M. T., & Menke, W. H. (2017). Seismic high attenuation region observed beneath southern new england from teleseismic body wave spectra: Evidence for high asthenospheric temperature without melt. *Geophysical Research Letters*, *44*(21). <https://doi.org/10.1002/2017GL074953>
- Duvernay, T., Davies, D. R., Mathews, C. R., Gibson, A. H., & Kramer, S. C. (2021). Linking intraplate volcanism to lithospheric structure and asthenospheric flow. *Geochemistry, Geophysics, Geosystems*, *22*(8). <https://doi.org/10.1029/2021GC009953>
- Eilon, Z., Fischer, K. M., & Dalton, C. A. (2018). An adaptive Bayesian inversion for upper-mantle structure using surface waves and scattered body waves. *Geophysical Journal International*, *214*(1), 232–253. <https://doi.org/10.1093/gji/ggy137>
- Ekström, G. (2017). Short-period surface-wave phase velocities across the conterminous United States [Dataset]. *Physics of the Earth and Planetary Interiors*, *270*, 168–175. <https://doi.org/10.1016/j.pepi.2017.07.010>
- Fischer, K. M. (2002). Waning buoyancy in the crustal roots of old mountains. *Nature*, *417*(6892), 933–936. <https://doi.org/10.1038/nature00855>
- Fulla, J., Lebedev, S., Martinec, Z., & Celli, N. L. (2021). WINTERC-G: Mapping the upper mantle thermochemical heterogeneity from coupled geophysical–petrological inversion of seismic waveforms, heat flow, surface elevation and gravity satellite data. *Geophysical Journal International*, *226*(1), 146–191. <https://doi.org/10.1093/gji/ggab094>
- Havlin, C., Parmentier, E. M., & Hirth, G. (2013). Dike propagation driven by melt accumulation at the lithosphere–asthenosphere boundary. *Earth and Planetary Science Letters*, *376*, 20–28. <https://doi.org/10.1016/j.epsl.2013.06.010>
- Hinze, W. J., & Chandler, V. W. (2020). Reviewing the configuration and extent of the Midcontinent rift system. *Precambrian Research*, *342*, 105688. <https://doi.org/10.1016/j.precamres.2020.105688>
- Hopper, E., & Fischer, K. M. (2018). The changing face of the lithosphere–asthenosphere boundary: Imaging continental scale patterns in upper mantle structure across the contiguous U.S. with Sp converted waves [Dataset]. *Geochemistry, Geophysics, Geosystems*, *19*(8), 2593–2614. <https://doi.org/10.1029/2018GC007476>
- Hopper, E., Fischer, K. M., Wagner, L. S., & Hawman, R. B. (2017). Reconstructing the end of the Appalachian orogeny. *Geology*, *45*(1), 15–18. <https://doi.org/10.1130/g38453.1>
- Incorporated Research Institutions for Seismology. (2010). Data services products: EARS EarthScope Automated Receiver Survey [Dataset]. *Incorporated Research Institutions for Seismology*. <https://doi.org/10.17611/DP/EARS.1>
- Jourdan, F., Marzoli, A., Bertrand, H., Cirilli, S., Tanner, L. H., Kontak, D. J., et al. (2009). <sup>40</sup>Ar/<sup>39</sup>Ar ages of CAMP in North America: Implications for the Triassic–Jurassic boundary and the 40K decay constant bias. *Lithos*, *110*(1–4), 167–180. <https://doi.org/10.1016/j.lithos.2008.12.011>
- Karato, S., Olugboji, T., & Park, J. (2015). Mechanisms and geologic significance of the mid-lithosphere discontinuity in the continents. *Nature Geoscience*, *8*(7), 509–514. <https://doi.org/10.1038/ngeo2462>

- King, S. D., & Ritsema, J. (2000). African hot spot volcanism: Small-scale convection in the upper mantle beneath cratons. *Science*, 290(5494), 1137–1140. <https://doi.org/10.1126/science.290.5494.1137>
- Krueger, H. E., Gama, I., & Fischer, K. M. (2021). Global patterns in cratonic mid-lithospheric discontinuities from Sp receiver functions. *Geochemistry, Geophysics, Geosystems*, 22(6), e2021GC009819. <https://doi.org/10.1029/2021gc009819>
- Levin, V., Long, M. D., Skryzalin, P., Li, Y., & López, I. (2018). Seismic evidence for a recently formed mantle upwelling beneath New England. *Geology*, 46(1), 87–90. <https://doi.org/10.1130/G39641.1>
- Levin, V., Servali, A., VanTongeren, J., Menke, W., & Darbyshire, F. (2017). Crust-mantle boundary in eastern North America, from the (oldest) craton to the (youngest) rift.
- Lin, A.-B., Aulbach, S., Zheng, J.-P., Cai, R., Liu, J., Xiong, Q., & Pan, S.-K. (2023). Lithospheric mantle provinces and crust-mantle decoupling beneath northeastern China: Insights from peridotite xenoliths. *GSA Bulletin*, 135(3–4), 990–1008. <https://doi.org/10.1130/B36338.1>
- Liu, D., & Chen, L. (2019). Edge-driven convection and thinning of craton lithosphere: Two-dimensional thermal-mechanical modeling. *Science China Earth Sciences*, 62(12), 2106–2120. <https://doi.org/10.1007/s11430-019-9371-0>
- Long, M. D., Benoit, M. H., Aragon, J. C., & King, S. D. (2019). Seismic imaging of mid-crustal structure beneath central and eastern North America: Possibly the elusive Grenville deformation? *Geology*, 47(4), 371–374. <https://doi.org/10.1130/G46077.1>
- Long, M. D., Wagner, L. S., King, S. D., Evans, R. L., Mazza, S. E., Byrnes, J. S., et al. (2021). Evaluating models for lithospheric loss and intraplate volcanism beneath the central Appalachian mountains. *Journal of Geophysical Research: Solid Earth*, 126(10). <https://doi.org/10.1029/2021JB022571>
- Lynner, C., & Bodmer, M. (2017). Mantle flow along the eastern North American margin inferred from shear wave splitting. *Geology*, 45(10), 867–870. <https://doi.org/10.1130/G38980.1>
- Lynner, C., Guajardo, A., Eilon, Z., & Janiszewski, H. A. (2019). Surface wave tomography across the Eastern North American Margin from amphibious data [Dataset]. *Surface wave tomography across the Eastern North American Margin from amphibious data* [Dataset], fall meeting 2019, abstract #T21F-0376 (Vol. 2019, pp. T21F-0376). Retrieved from <https://ui.adsabs.harvard.edu/abs/2019AGUFM.T21F0376L/abstract>
- Lynner, C., & Porritt, R. W. (2017). Crustal structure across the eastern North American margin from ambient noise tomography [Dataset]. *Geophysical Research Letters*, 44(13), 6651–6657. <https://doi.org/10.1002/2017GL073500>
- Mazza, S. E., Gazel, E., Johnson, E. A., Bizimis, M., McAleer, R., & Biryol, C. B. (2017). Post-rift magmatic evolution of the eastern North American “passive-aggressive” margin. *Geochemistry, Geophysics, Geosystems*, 18(1), 3–22. <https://doi.org/10.1002/2016GC006646>
- Mazza, S. E., Gazel, E., Johnson, E. A., Kunk, M. J., McAleer, R., Spotila, J. A., et al. (2014). Volcanoes of the passive margin: The youngest magmatic event in eastern North America. *Geology*, 42(6), 483–486. <https://doi.org/10.1130/G35407.1>
- Menke, W., Lamoureaux, J., Abbott, D., Hopper, E., Hutson, D., & Marrero, A. (2018). Crustal heating and lithospheric alteration and erosion associated with asthenospheric upwelling beneath southern New England (USA). *Journal of Geophysical Research: Solid Earth*, 123(10), 8995–9008. <https://doi.org/10.1029/2018JB015921>
- Menke, W., Skryzalin, P., Levin, V., Harper, T., Darbyshire, F., & Dong, T. (2016). The northern Appalachian anomaly: A modern asthenospheric upwelling. *Geophysical Research Letters*, 43(19), 1–7. <https://doi.org/10.1002/2016GL070918>
- Miller, S. R., Sak, P. B., Kirby, E., & Bierman, P. R. (2013). Neogene rejuvenation of central Appalachian topography: Evidence for differential rock uplift from stream profiles and erosion rates. *Earth and Planetary Science Letters*, 369–370, 1–12. <https://doi.org/10.1016/j.epsl.2013.04.007>
- Mosher, S. (1998). Tectonic evolution of the southern Laurentian Grenville orogenic belt. *Geological Society of America Bulletin*, 110(11), 1357–1375. [https://doi.org/10.1130/0016-7606\(1998\)110<1357:teotsl>2.3.co;2](https://doi.org/10.1130/0016-7606(1998)110<1357:teotsl>2.3.co;2)
- Murphy, B. S., & Egbert, G. D. (2019). Synthesizing seemingly contradictory seismic and magnetotelluric observations in the southeastern United States to image physical properties of the lithosphere. *Geochemistry, Geophysics, Geosystems*, 20(6), 2606–2625. <https://doi.org/10.1029/2019GC008279>
- Nettles, M., & Dziewoński, A. M. (2008). Radially anisotropic shear velocity structure of the upper mantle globally and beneath North America. *Journal of Geophysical Research*, 113(B2), 2006JB004819. <https://doi.org/10.1029/2006JB004819>
- Petruska, J., & Eilon, Z. (2022). Distributed extension across the Ethiopian rift and plateau illuminated by joint inversion of surface waves and scattered body waves. *Geochemistry, Geophysics, Geosystems*, 23(3). <https://doi.org/10.1029/2021GC010179>
- Ramsalou, T., & Pysklywec, R. (2011). Anomalous bathymetry, 3D edge driven convection, and dynamic topography at the western Atlantic passive margin. *Journal of Geodynamics*, 52(1), 45–56. <https://doi.org/10.1016/j.jog.2010.11.008>
- Saha, S., Peng, Y., Dasgupta, R., Mookherjee, M., & Fischer, K. M. (2021). Assessing the presence of volatile-bearing mineral phases in the cratonic mantle as a possible cause of mid-lithospheric discontinuities. *Earth and Planetary Science Letters*, 553, 116602. <https://doi.org/10.1016/j.epsl.2020.116602>
- Savage, B. (2021). Body wave speed structure of eastern North America. *Geochemistry, Geophysics, Geosystems*, 22, 1–18. <https://doi.org/10.1029/2020GC009002>
- Schmandt, B., & Lin, F. (2014). P and S wave tomography of the mantle beneath the United States. *Geophysical Research Letters*, 41(18), 6342–6349. <https://doi.org/10.1002/2014GL061231>
- Schutt, D. L., & Leshner, C. E. (2006). Effects of melt depletion on the density and seismic velocity of garnet and spinel lherzolite. *Journal of Geophysical Research*, 111(B5). <https://doi.org/10.1029/2003JB002950>
- Selway, K., Ford, H., & Kelemen, P. (2015). The seismic mid-lithosphere discontinuity. *Earth and Planetary Science Letters*, 414, 45–57. <https://doi.org/10.1016/j.epsl.2014.12.029>
- Shen, W., & Ritzwoller, M. H. (2016). Crustal and uppermost mantle structure beneath the United States [Dataset]. *Journal of Geophysical Research: Solid Earth*, 121(6), 4306–4342. <https://doi.org/10.1002/2016JB012887>
- Stein, S., Stein, C. A., Elling, R., Kley, J., Keller, G. R., Wyssession, M., et al. (2018). Insights from North America’s failed Midcontinent Rift into the evolution of continental rifts and passive continental margins. *Tectonophysics*, 744, 403–421. <https://doi.org/10.1016/j.tecto.2018.07.021>
- Tao, Z., Li, A., & Fischer, K. M. (2021). Hotspot signatures at the North American passive margin. *Geology*, 49(5), 525–530. <https://doi.org/10.1130/G47994.1>
- Tesauro, M., Kaban, M. K., & Mooney, W. D. (2015). Variations of the lithospheric strength and elastic thickness in North America. *Geochemistry, Geophysics, Geosystems*, 16(7), 2197–2220. <https://doi.org/10.1002/2015GC005937>
- Thomas, W. (2006). Tectonic inheritance at a continental margin. *Geological Society of America Today*, 16(3), 4–11. [https://doi.org/10.1130/1052-5173\(2006\)016\[4:TIAACM\]2.0.CO;2](https://doi.org/10.1130/1052-5173(2006)016[4:TIAACM]2.0.CO;2)
- Turcotte, D., & Schubert, G. (2014). *Gynamics* (3rd ed., Vol. 40(6)). Retrieved from [http://doi.wiley.com/10.1002/1521-3773\(20010316\)40:6%3C9823::AID-ANIE9823%3E3.3.CO;2-C](http://doi.wiley.com/10.1002/1521-3773(20010316)40:6%3C9823::AID-ANIE9823%3E3.3.CO;2-C)

- Wagner, L. S., Fischer, K. M., Hawman, R., Hopper, E., & Howell, D. (2018). The relative roles of inheritance and long-term passive margin lithospheric evolution on the modern structure and tectonic activity in the southeastern United States. *Geosphere*, *14*(4), 1385–1410. <https://doi.org/10.1130/GES01593.1>
- Whitmeyer, S. J., & Karlstrom, K. E. (2007). Tectonic model for the Proterozoic growth of North America (Vol. 40).
- Withjack, M. O., Schlische, R. W., & Olsen, P. E. (2012). Development of the passive margin of Eastern North America. In *Regional geology and tectonics: Phanerozoic rift systems and sedimentary basins* (Vol. 6, pp. 300–335). Elsevier. <https://doi.org/10.1016/B978-0-444-56356-9.00012-2>
- Yamauchi, H., & Takei, Y. (2016). Polycrystal anelasticity at near-solidus temperatures. *Journal of Geophysical Research: Solid Earth*, *121*(11), 7790–7820. <https://doi.org/10.1002/2016JB013316>